Applied Energy 162 (2016) 460–471

Contents lists available at ScienceDirect

Applied Energy

journal homepage: www.elsevier.com/locate/apenergy

A passive cooling wind catcher with heat pipe technology: CFD, wind tunnel and field-test analysis

John Kaiser Calautit *, Ben Richard Hughes

Department of Mechanical Engineering, University of Sheffield, Sheffield S10 2TN, UK

HIGHLIGHTS

- A cooling wind tower incorporating heat pipe technology and cool sink was proposed.
- A cooling potential of up to 12 °C of air streams was identified in this study.
- Significant reduction in the temperature was observed at lower wind speeds (1–2 m/s).
- The system met the recommendation (10 L/s/person) for a wind speed of 2 m/s and higher.
- Field testing was carried out in Ras Al Khaimah, UAE to evaluate its performance under real operating conditions.

GRAPHICAL ABSTRACT

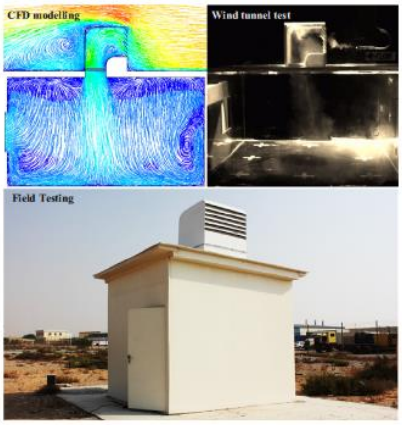

Abstract

Wind catchers are natural ventilation systems based on the design of traditional architecture, intended to provide ventilation by manipulating pressure differentials around buildings induced by wind movement and temperature difference. Though the movement of air caused by the wind catcher will lead to a cooling sensation for occupants, the high air temperature in hot regions will result in little cooling to occupants. In order to maximise the properties of cooling by wind catchers, heat pipes were incorporated into the design. Computational Fluid Dynamics (CFD) was used to investigate the effect of the cooling devices on the performance of the wind catcher, highlighting the capabilities of the system to deliver the required fresh air rates and cool the ventilated space. Qualitative and quantitative wind tunnel measurements of the airflow through the wind catcher were compared with the CFD data and good correlation was observed. Preliminary field testing of the wind catcher was carried out to evaluate its thermal performance under real operating conditions. A cooling potential of up to 12 ˚C of supply air temperature was identified in this study.

Keywords: field study; hot climate; numerical analysis; passive cooling; wind tunnel

1. Introduction

At present the construction, operation and maintenance of the building sector makes up as much as 40% of global energy demand as well as 40-50 % of the global carbon emissions [1]. Heating Ventilation and Air Conditioning (HVAC) systems consume more than 60 % of the total energy use of buildings [2]. In hot climates, such as those in Middle East countries, the percentage of energy consumption by air conditioning (AC) is significantly larger due to the more extreme conditions of the local climate [3]. In 2005, the average Watt/person in the Gulf Cooperation Council (GCC) countries was 1149 Watt/person which was much greater than the world average (297 Watt/person) [4]. In addition to this, the rapid growth of the development of infrastructure had increased the energy consumption at a faster rate. The solution to this problem, though, might be closer to home than previously thought. Architects and building engineers are currently looking at traditional gulf architecture as a way of providing passive cooling and acceptable indoor environmental quality for modern buildings, not just in the Middle East but around the globe. The wind catcher concept has been around for centuries and is common feature in the Middle Eastern architecture [5]. Figure 1 illustrates different forms of traditional wind catcher systems in Iran. Modern wind catchers have been available in the UK for the last forty years; recent rising energy costs have seen their implementation into new and existing buildings increase [6].

Figure 1 Different forms of traditional wind catcher architecture [5].

The wind catcher sustain natural ventilation through indoor space spaces through wind driven airflow as well as buoyancy effect. Wind catchers are typically a tall structure projecting on top of the roof of a building [7]. This allows the wind catcher to capture air at a higher velocity and supply it into the space. Furthermore, it can also provide night time cooling by removing the heat stored in the building fabric thereby moderating internal daytime temperatures.

Though the movement of air caused by the wind catcher over exposed skin will lead to a cooling sensation for occupants, the high air temperature in hot climates will result in little cooling to occupants [8]. Therefore, wind catchers are integrated with evaporative cooling techniques such as wetted surfaces, fountains and ground cooling [9] to enhance the cooling by the device. However, there are few issues associated with evaporative cooling such as high operation and maintenance cost [10]. Evaporative coolers use a substantial amount of water to run. Hence, this should be taken into consideration in areas where water is expensive

or in short supply. In some areas, discarded water from the cooling tower can be an environmental concern. Furthermore, evaporative cooling towers use wet surface or nozzles to add water vapor into the air. These wet surfaces should be cleaned regularly to avoid mold and bacteria. Other drawbacks associated with the evaporative cooling towers are discussed in [10].

The proposed wind catcher presented in this study uses heat transfer devices involving heat pipes to provide a continuous cooling loop (Figure 2). A heat pipes is a device of high thermal conductivity with no moving parts that can efficiently transfer large quantities of heat over large distances fundamentally at an invariable temperature without any electrical input. It is also more compact and a viable alternative for modern wind catchers which are smaller compared to traditional systems. It is composed of three sections: the evaporator, where heat from the incoming air is absorbed; the adiabatic section in between; and condenser, where heat is rejected to a parallel closed-circuit cool sink [10]. Unlike the evaporative cooling tower which directly sprays water and add moisture into the airstream, the water from the cool sink never comes in direct contact with the conditioned supply air. Therefore, there is less increase in moisture content compared to evaporative cooling techniques, hence, making it also viable for moderate humid conditions and there is less risk of contamination of the airstream.

Figure 2 Cooling wind catcher with heat pipes.

In our earlier work [10], we've investigated the integration of heat pipes into a traditional wind catcher using CFD modeling. The analysis showed the application of heat pipes for natural ventilation cooling. The work concluded that the system was capable of reducing the air temperature by up to 12-15 ˚C. The conclusions were based completely on the results of the CFD analysis, therefore further research (experimental test) was required. Furthermore, we've also investigated the integration of the heat pipes into a commercial wind catcher [11]. The results showed the capability of the system in supplying the recommended fresh air rates following the addition of the cooling devices. Likewise, the study was completely CFD-based and experimental testing of the proposed system was of further interest. Therefore, the aim of this work was to address the gap in the literature detailed above by performing laboratory and field test analysis. The results of this work will highlight the effectiveness of the wind catcher under real operating conditions and the obtained data will be useful for its further development.

2. Previous Related Works

A number of studies have investigated the integration of evaporative cooling into a wind catcher. Badran [12] assessed the performance of an wind catcher with evaporative cooling. An analytical model was developed for the analysis of the effect of outdoor wind conditions on the airflow passing through the evaporative cooling columns. The results showed that a 4 m wind catcher generated an airflow of 0.3 m^3/s and reduce the temperature by 11 ˚C.

Bahadori *et al.* [13] compared the performance of two wind catchers with evaporative cooling provisions. The tests were conducted in the city of Yazd, Iran during the month of September. The two wind catchers were one with wetted curtains inside the channel and the other one with cooling pads at the opening. The results showed that the wind catcher with curtains performed better during high wind speeds while the wind catcher with cooling pads performed better during low wind speeds. The study also confirmed that the addition of cooling device reduced the airflow through the wind catcher and increase the relative humidity.

The ability of the wind catcher to cool the incoming air was significant when evaporative cooling spray was integrated into the design. Yaghoubi *et al.* [14] provided a similar analysis which aligned with the measurements and conclusion drawn by Bahadori. Bouchahm *et al.* [15] performed experimental testing of a similar wind catcher but added a water pool at the bottom for enhanced cooling.

Safari and Hosseinnia [16] used CFD modeling to investigate the effect of the height of the wetted curtains on the evaporative cooling performance of the wind catcher developed by Bahadori *et al.* [13]. The CFD model which implemented the Eulerian-Lagrangian approach was validated against the analytical solutions of [13] and there was a good agreement between both methods. The results showed that the wetted curtains with the height of 10 m was able to cool the air by 12 ˚C.

A few studies have investigated the integration of heat pipes into natural ventilation systems. Shao and Riffat [17] were the first to investigate the use of heat pipes in passive ventilation, however the purpose of the system was to recover the heat from the exhaust stream. The numerical and experimental test showed that for a heat recovery efficiency of 50% and flow speed of 0.5 m/s, the pressure loss across the heat pipes was only 1 Pa. The work concluded that heat pipes do not create a significant pressure drop compared to other technology, this

was critical in the integration into passive ventilation systems as pressure losses should be kept to a minimum.

Calautit *et al.* [10, 11] also integrated heat pipes in a natural ventilation device but for cooling buildings in hot climates. The geometry of the device was based on the traditional wind catcher studied by Kalantar [18]. The evaporative cooling spray was replaced with heat pipes to compare the performance of a wind catcher with direct and indirect evaporative cooling. The CFD results showed that the temperature reduction of the air reached up to 12 ˚C for a pressure loss of only 5Pa.

To this end, the studies on commercial wind catcher with heat pipes for cooling were completely CFD based and the current work will expand the literature by carrying out wind tunnel testing and also field testing for proof of concept.

3. Research Methodology

Figure 3 shows a flow chart of the full assessment methodology for the evaluation of the performance of the wind catcher.

Figure 3 Research methodology flow chart.

3.1 CFD modelling and simulation

A commercial general purpose CFD code ANSYS FLUENT14 was used in this study to simulate the airflow inside the wind catcher model and into to the small room connected to it. The simulation was conducted at steady state and with a three-dimensional computational model. The CFD code used the Finite Volume Method (FVM) with the Semi Implicit Method for Pressure Linked Equations (SIMPLE) velocity-pressure coupling algorithm. Second order upwind schemes were adopted for the calculation. The turbulent component of the airflow was modeled using the standard k-ε turbulence model [19, 20]. Convergence was monitored and iterations were ended when all residuals showed no further reductions with increasing number of iterations. The governing equations are fully detailed in the ANSYS FLUENT Guide [21].

3.1.1 Design geometry and mesh generation

The wind catcher geometry (Figure 4a) was created using the commercial CAD software Solid Edge. The wind catcher was modelled with seven louvers angled at 45° and spaced at 0.1 m between each opening louvers. The top and bottom louvers connect the structure and do not allow airflow through. The cylindrical heat pipes, each with an outer diameter of 0.02 m, were integrated in to the lower part of the wind catcher channel. The spacing between the

heat pipes was 0.05 m (horizontal) and 0.02 m (vertical). The heat pipe dimension and spacing were based on an earlier study [22], which investigated the effect of various heat pipe pitch spacing on its thermal performance. The wind catcher was centrally placed above a small room or ventilated space with the height, width, and length of 3 m x 5 m and 5 m. The purpose of this was to investigate the capability of the device in ventilating and cooling an internal space. An enclosure or macro-climate which represents the external airflow was created around the wind catcher model. The macro-climate consisted of an inlet on one side of the domain, and an outlet on the opposing boundary wall. The distance between the wind catcher and the walls of the macro-climate was determined by calculating the blockage produced by the wind catcher. The dimension of the macro-climate was 5 m x 5 m x 10 m. According to the dimensions of the wind catcher (1 m x 1 m x 1 m), the model produced a maximum blockage of 4.8 %, therefore no corrections were made to the measurements obtained with these configurations [23].

The CAD data was imported into ANSYS Design Modeller (FLUENT pre-processor) and the fluid volumes were extracted from the solid CAD assembly. Due to the complexity of the geometry, an unstructured mesh was used to discretise the surface and volumes of the computational domains [19, 20]. To be able to capture properly the flow fields near the critical areas of interest in the simulation such as the heat pipes and louvers, size functions were applied in those surfaces. The size of the mesh element was extended smoothly to resolve the sections with high gradient mesh and to improve the accuracy of the results of the velocity and temperature fields [23, 24]. The mesh element size was varied from 0.005 m for the mesh near the heat transfer devices and louvers to 0.07 m for the middle of the space. Figure 4b shows the meshing of the modeled wind catcher and room using ANSYS Mesh. The total number of the mesh elements was equal to 3.75 million.

Figure 4 (a) CAD model of the wind catcher with cylindrical heat pipes (b) Computational mesh of the wind catcher and test room model.

The verification of mesh was performed by mesh sensitivity analysis on different mesh sizes. The mesh verification method starts with a coarse mesh and gradually refines it until the variation observed between the results were smaller than the predefined acceptable error. The accuracy of the results was improved by using successively smaller cell sizes for the computation [23, 24]. The velocity distribution inside the room model with a simulation set-up of different mesh sizes was evaluated with an external wind speed of 3 m/s and angle of 0˚. The set boundary conditions remained fixed throughout the process to ascertain precise

comparison of the results. The initial coarse grid consisted of 2,674,484 elements which was refined over five stages until an acceptable error of 0.1 % was achieved with a total of 7,249,235 elements.

3.1.2 CFD Boundary conditions

Figure 5 shows the computational domain containing the macro- and micro-climate volumes. A wall boundary condition was used to create a boundary between each region. The macro-climate fluid volume was used to simulate the external velocity of the flow field. In order to generate velocity for the flow, a vertical wall was used as a velocity inlet, while the opposite boundary wall was set as the pressure outlet. To reveal the characteristics of the natural ventilation wind catcher, the simulations were conducted with wind speeds between 0.5 and 5 m/s. The external air temperature was set to 45 °C to simulate a hot external environment. The wall temperature of the heat pipes was set to 20 °C [25].

Figure 5 Computational domain showing the set boundary conditions.

3.2 Scaled wind tunnel testing

The test setup for the wind tunnel experiment was designed to replicate the CFD modeling of the wind catcher as seen in Figure 5. A low-speed wind tunnel (Figure 6) was used for the experiment and is detailed in [26]. The test section of the wind tunnel with the dimensions of 0.5 m, 0.5 m, and 1 m represent the macro-climate. A 0.1 m x 0.1 m opening at the bottom of the test section was used to position the wind catcher inside the test section. A small box represents the micro-climate was located beneath the test section as shown in Figure 7b. Similar to the CFD model, the experimental model of the wind catcher produced a blockage of 4.8 % inside the test section. The geometric scale of the model of the wind catcher was selected to maintain, as close as possible, equality of model and prototype ratios of overall dimensions to the important meteorogical lengths of the simulated wind. All the relevant dimensions of the prototype were equally scaled down by the appropriate factor [27].

Figure 6 Wind tunnel test setup.

Due to the size of the required experimental model (1:10 scale) and complexity of the wind catcher geometry, the wind tunnel model was created using a 3D printer. The 3D printer uses the Fused Deposition Modelling (FDM) or additive manufacturing process. FDM builds the three dimensional parts by melting and advancing a fine ribbon of acrylonitrile butadiene styrene (ABS) plastic through a computer-controlled extrusion head. From the 3D CAD data, the pre-processing software processes the STereoLithography (STL) file by creating sliced

layers of the model, calculates support structures and creates tool paths that are optimised for the rapid prototyping machine The rapid prototyping machine forms the item by depositing the material (ABS plastic) in layers through a computer controlled extrusion head, starting with the bottom layer, onto a platform. Dual extrusion heads precisely lay down thermo-plastic model and support material to create each layer. Temporary support structures are removed. Soluble support material automatically dissolves in a water-based solution.

Cylindrical rods with an outer diameter of 0.002 m were used to model the heat pipes inside the wind catcher. The bottom section of the wind tower was printed as a separate model with the heat pipes hole patterns so that the cylindrical rods can be easily slotted in. This will ensure that the distance between the cylindrical heat transfer devices are matching simulation model. The wind catcher model in Figure 7a was connected to a 0.5 m x 0.5 m x 0.3 m room (Figure 7b). A 0.1 m x 0.1 m opening at the leeward side of the room represents the outlet. The room model was made of clear perspex sheets to allow the accurate positioning of the measurement sensors inside the room. The top plate of the room was constructed that it could be rotated in the test section in order to test different approaching wind directions.

Figure 7 (a) Schematic diagram of the wind catcher with cylindrical heat pipes (b) test room.

The airflow into the room was measured using a hot-wire anemometer positioned below the channels of the wind catcher. The cross-sectional area of the wind catcher channel was divided into several portions and the airflow rate through the channel was calculated. Figure 8a shows the position of the measurement points inside the channel at a height of 0.27 m from the base of the room. The hot-wire anemometer gave airflow velocity measurements with uncertainty of ±1.0 % rdg. at airflow velocity lower than 8 m/s and uncertainty of ±0.5 % rdg. at airflow velocity higher than 8 m/s. Time averaging was conducted for a period of 2 minutes to obtain a statistical value. Additionally, smoke testing was also conducted to visualise the airflow pattern in and around the wind catcher and the room model. The AFA10 smoke generator and high speed camera (523 fps) was used for the smoke visualisation and recording.

Figure 8 (a) Location of measurement points below the wind catcher channel (b) hot-wire anemometer.

3.3 Field test site and data collection

Preliminary field testing of the cooling wind catcher was carried out to evaluate its thermal performance under real operating conditions. A full-scale prototype of the cooling wind catcher was produced and installed on top of an unoccupied 3 m x 3 m x 3 m room on an open field site in Ras Al Khaimah, United Arab Emirates (UAE). Figure 9 shows the site location and the test setup. Ras Al Khaimah is the northern part of UAE, located at latitude 25.78˚N and longitude 55.95 ˚E. The climate of Ras Al Khaimah can be characterised as a hot-desert climate. High temperatures can be expected from June to September, with a maximum temperature ranging between 39 ˚C and 42 ˚C and a minimum temperature ranging between 24 ˚C and 30 ˚C. Figure 10 shows the weather statistics for the city of Ras Al Khaimah [28]. The predominant wind direction is between N and N-W direction [28]. Therefore, the opening of the wind catcher was positioned to face the predominant wind. The average wind speed is between 4 m/s and 5 m/s [28].

The field tests were carried out during the month of September (September 18 and 19, 2014). The tests were conducted during the day between 11:00 AM and 4:00 PM (highest outdoor air temperatures). The wind catcher was mounted on top of the test room which was constructed from insulated studwork (weather-proofed). An opening located on the leeward side of the room was used as an outlet. The prototype of the wind catcher (see Figure 2) was constructed using aluminum plate with a thickness of 3 mm. The overall dimension of the wind catcher was 1 m x 1 m x 1.2 m. A total of 50 cylindrical heat pipes (each with an outer diameter of 0.02 m and total length of 0.95 m) and a parallel cold sink (fed by water at approximately 15 ˚C - 20 ˚C) were incorporated into the wind catcher to provide the cooling. Similar to the CFD and wind tunnel model, the heat pipes were arranged in a staggered grid with a stream wise distance of 0.02 m and a span wise distance of 0.05 m.

Figure 9 Field test site in Ras Al Khaimah, UAE.

Type K thermocouples (exposed tip, PTFE insulated) and a multi-channel data logger were used to monitor and collect the temperature data. The thermocouple had a tip diameter of 1.5 mm and a tip temperature range between −75 °C and 250 °C. Based on the recent calibration certificate provided by the manufacturer, the maximum allowable measurement uncertainty of the device at 0 °C was 0.5 °C and 0.6 °C at a temperature of 50 °C. It is worth noting that additional uncertainty analysis was also performed by comparing the temperature measurements of the test thermocouples with a reference thermocouple. The external air, supply air (below the wind catcher channel) and heat pipe surface temperatures were monitored with the thermocouple. Data were recorded on a continuous basis with a sampling

period of 1 sec. The external conditions were monitored using an outdoor weather station equipped with temperature and wind measurement devices. The weather station was located 50 meters away from the test site and its sensors were 5 meters above the ground.

Figure 10 Weather data of Ras Al Khaimah, UAE [28].

4. Results and Discussion

4.1 Comparison between wind tunnel and computational data

Comparison between the predicted and experimental results for the airflow velocity measurements are presented in Figure 11a. An uneven airflow distribution was observed below the supply channel. The airflow speed on the right corner of the channel (Points 1, 4 and 7) was 30 – 60 % higher than the left corner (Points 3, 6 and 9). This was due to the flow separation created by the sudden change in direction (90˚ bend) inside the wind catcher and also the acceleration of the flow near the leeward wall. Good agreement was observed between the CFD results and wind tunnel measurement, with the error under 10 % for all the points except for point 6. This point was located near the recirculation region inside the wind catcher (See Figure 12). This is one of the limitations of the k-epsilon turbulence model which does not perform well in cases of complex flows. This was also evident with point 3 (3.27% error) and point 9 (5.08%) which were also close to the recirculation region inside the wind catcher. The average error across the points was 7.2 %. Using the recommended justification [29], it can be claimed that the validation of the CFD modeling study was acceptable. Overall, the trend (points 1 -9) showed that the CFD model was capable of predicting the supply airflow.

Figure 11b compares the CFD and experimental results of the volumetric airflow through the wind catcher channel at different wind directions (0˚ to 90˚). The predominant wind stream (0˚) caused the maximum flow rate at entrance of the wind catcher. Increasing the angle reduced the operation of the wind catcher and the minimum operation was observed at the transition angle (> 70°). Angles larger than the transition angle caused a change in the direction of the airflow. Exposing the body of the wind catcher on the path of the airflow caused a low pressure region on its back and sides. Positioning its opening in this region with a lower pressure than the indoor, resulted in an airflow from the window to the opening of the wind catcher (suction).

Figure 11 (a) Comparison between CFD and experimental results of the (a) velocity in the supply channel (b) effect of variation of wind direction on the supply flow rate.

Figure 12 shows a comparison of the flow patterns inside the test room model between the smoke visualisation and CFD. At the point of entry (below the wind catcher), there was a higher density of smoke suggesting higher air speeds at this part of the room. After entry, the airflow directly hit the floor of the test room. Lower air speed was observed at this point, the air then spread sideways and upwards in all direction and part of it escaped through the outlet located on the left wall. A region of highly unsteady and recirculating flow was observed immediately at the downstream of the wind catcher.

Figure 12 CFD streamlines showing indoor airflow distribution

Video 1 Experimental flow visualisation inside the test room with the wind catcher.

4.2 Velocity distribution

In figure 13a, the CFD simulation results of the velocity distribution inside the cooling wind catcher and macro-micro climate are displayed. The left hand side of the figure shows the scale of airflow velocity (m/s). The contour plot in the fluid domain is colour coded and related to the colour map, ranging from 0 to 3.8 m/s. The external air was flowing around the wind catcher from the right side of the macro-climate domain, parts of it entered the wind catcher and parts of it flowed out through the left side of the domain. The airflow entering the wind catcher was accelerated at it passed through the 90˚ bend, reaching a maximum speed of 1.7 m/s near the outer wall of the bend. Separation occurred near the internal wall of the sharp turn as the flow encounters adverse pressure gradients that was developed in that region. The airflow was re-directed downwards and a significant reduction in speed was observed downstream of the heat pipes. In the micro-climate, airflow velocity ranged from 0.11 to 0.83 m/s under conditions where the external air velocity was 3 m/s. The air stream was circulated inside the space and exhausted out from the opening located on the leeward side of the micro-climate. Figure 13b shows the relation between the varying external wind speeds and performance of the wind catcher in terms of the internal airflow distribution.

Figure 13 (a) Contours of airflow velocity in vertical cross-sectional plane (b) effect of increasing wind speed on internal airflow distribution.

4.3 Ventilation rate

In Table 1, the ventilation rates obtained by simulation of different outdoor wind speeds are summarised. The Building Regulations Approved Document F for ventilation suggested that ventilation rate of 10 L/s per occupant was recommended for classrooms spaces [30] and this was achieved by the system when the external wind speeds was higher than 1 m/s. It was assumed that there were 15 occupants in the micro-climate with a floor area of 25 m^2 [31, 32]. Based on our previous work [24], increasing the wind tower supply rate from 135 L/s to 405 L/s can reduce the average CO_2 concentration from 845 ppm to 555 ppm inside a room occupied by 15 people.

Table 1 Calculated ventilation rates for various external wind speeds.

4.4 Temperature distribution

Figure 14 illustrates the temperature distribution obtained by CFD simulation. The right hand side of the contour plot shows the scale of air temperature (˚C). The contour plot in the fluid domain is colour coded and related to the CFD colour map, ranging from 20 ˚C to 45 ˚C. From the right-hand side of the domain, external hot air at 45 ˚C flowed into the wind catcher and into the micro-climate. The air temperature was reduced at the immediate downstream of the heat pipe arrangement with a calculated temperature reduction of 8.8 ˚C. In the micro-climate, airflow temperature ranged from 33 ˚C to 40 ˚C under conditions where the external air velocity and temperature was 3 m/s and 45 ˚C. Figure 15 shows the effect of varying external wind speeds (1 – 5 m/s) on the thermal performance of the wind catcher. The temperature reduction increased as the wind speed decreased due to the increase in contact time between the external airstream and the heat pipes. Conversely, the temperature reduction was shown to decrease at increasing external wind speeds. For instance, at 5 m/s wind speed, the temperature was only reduced by 5 ˚C. Significant reduction in temperature was observed at lower wind speeds (1 m/s – 2 m/s), up to 9.5 ˚C – 12 ˚C reduction.

Figure 14 Contours of airflow temperature in vertical cross-sectional plane.

Figure 15 Effect of increasing wind speed on internal and supply air temperature.

4.5 Field test results

Figure 16a shows the speed and direction of the wind from 11:00 AM to 4:00 PM (1 hour sampling period). From 11:00 AM to 12:00 PM, the wind was mostly blowing from the SW to WSW direction (90˚ to 112.5˚ approach angle). The analysis of the effect of wind direction of the airflow rate in Figure 14b showed that when the approach angle exceeded 70˚, the

airflow into the wind catcher began to change direction. In this situation, the wind catcher was acting as an exhaust devices and the air was entering from the window to the opening of the wind catcher. From 12:00 PM to 1:00 PM, the wind started to blow from the WNW direction (45˚ approach angle) and the wind catcher began to deliver airflow into the room. At 45˚ approach angle, the wind catcher supplies airflow at a reduced rate as observed in Figure 14b. From 2:00 PM to 4:00 PM, the wind catcher was mostly on the route of the predominant wind stream (0˚ to 10˚ approach angle) and caused maximum entrance flow rate into the wind catcher. The wind speed varied between 3 m/s and 6 m/s.

Figure 16b is an example of the day-time cooling of the system during a windy-summer day. It shows the external air temperature, heat pipe surface temperature and the temperature downstream of the heat pipes (measured at three separate points) as a function of time. The cold sink was fed with water every 15 – 20 minutes to maintain the sink temperature at around 20 ˚C. This was initiated when the wind catcher began to deliver airflow inside the room (11:40 AM), although the wind was still mostly out from the W direction at this point. The air temperature decreased by 3 ˚C - 4 ˚C at 12:00 PM when the wind started to flow inside the wind catcher. It is worth noting that continuous airflow and sufficient temperature difference between the supply channel and cool sink are required for continuous cooling. Hence, alternating airflow direction could reduce the performance. At 1:00 PM, the wind was blowing more consistently from WNW direction (45˚ approach angle) and the reduction was 4 ˚C - 5 ˚C. From 2:00 to 4:00 PM, the wind was parallel to the opening of the wind catcher and the temperature reduction ranged between 2 ˚C - 7 ˚C. Figure 16c shows a zoomed in view of the temperature measurements from 3:00 PM to 3:30 PM.

Figure 17a shows the speed and direction of the wind from 11:00 AM to 4:00 PM, September 18, 2014. The wind speed varied between 1.5 m/s and 5.8 m/s, which was lower compared to the previous day. Similarly, the wind direction was blowing opposite (SW – SE) from the wind catcher opening during the start of the test. The wind catcher began to deliver airflow into the room at 11:30 AM and the temperature reduction ranged between 3 ˚C - 4 ˚C (Figure 17b). From 1:00 to 4:00 PM, the wind was blowing mostly from NW and NNE direction and the temperature reduction ranged between 3 ˚C – 11.5 ˚C. Figure 17c shows a zoomed in view of the temperature measurements from 3:00 PM to 3:30 PM.

Figure 16 September 17, 2014 testing: (a) Wind speed and direction (b) Heat pipe surface, outdoor air and supply air temperature (c) temperature results from 3:00 PM to 3:30 PM.

Figure 17 September 18, 2014 testing: (a) Wind speed and direction (b) Heat pipe surface, outdoor air and supply air temperature (c) temperature results from 2:30 PM to 3:00 PM.

5. Conclusion

The integration of natural ventilation wind catchers as a low energy alternative to mechanical HVAC systems or as a support to it (i.e. hybrid system) has the potential to improve the indoor air quality (IAQ) and reduce CO_2 emissions by reducing reliance on energy-intensive HVAC. From the review of previous works, it was concluded that cooling the temperature of supply air through a low energy technology such as heat pipes still remains incomplete. Therefore, this study addressed this by performing CFD simulation, wind tunnel analysis and field testing of a wind catcher with heat pipes. The CFD model provided detailed analysis of the airflow distribution inside the wind catcher and also the space that was being ventilated. The wind catcher was able to supply the ventilation rates recommended by the Building Regulations even at low outdoor wind speeds. A cooling potential of up to 12 ˚C of indoor air temperature was identified in this study. Simulation of various external wind speeds (1-5 m/s) showed that the cooling performance of the heat transfer device was indirectly proportional to the air supply rate. At 5 m/s external air speed, the air temperature was only reduced by 5 - 6 ˚C. While, higher temperature reduction was observed at lower wind speed, 9.5 ˚C reduction at 2 m/s. Qualitative and quantitative wind tunnel measurements of the airflow were compared with the CFD data. The difference between the results was 10 % on average. Full-scale field testing of the wind catcher was carried out to evaluate its thermal performance under real operating conditions. The field test demonstrated the positive effect of the addition of heat pipes on the cooling performance but also revealed technical issues which remain to be solved such as airflow control strategy and cool sink operation. Furthermore, the potential of the wind catcher working in combination with active systems such as smaller ac units (i.e. hybrid operation) should be further explored. Addition of fins and variation of the heat pipe spacing, arrangement, and sizing to optimise the cooling and natural ventilation performance is of further interest. Further testing of the wind catcher is also required to characterise its full year operation.

Acknowledgement

The support by the University of Leeds and CSEM-UAE are gratefully acknowledged. The statements made herein are solely the responsibility of the authors. The technology presented here is subject to an international patent application (PCT/GB2014/052263).

Reference

[1] M.M. Rahman, M.G. Rasul and M.M.K. Khan, "Energy conservation measures in an institutional building in sub-tropical climate in Australia," **Applied Energy**, vol. 87, pp. 2994-3004, 2010.

[2] Y.H. Yau and S.K. Lee, "Feasibility study of an ice slurry-cooling coil for HVAC and R systems in a tropical building," **Applied Energy**, vol. 87, Issue 8, pp. 2699-2711, 2010.

Sofotasiou P, Hughes BR, Calautit JK, Qatar 2022: Facing the FIFA World Cup climatic and legacy challenges, **Sustainable Cities and Society,** 2015, 14, 16-30.

[3] P. Sofotasiou, B. R. Hughes and J. K. Calautit, "Qatar 2022: Facing the FIFA World Cup climatic and legacy challenges," **Sustainable Cities and Society,** vol. 14, pp. 16-30, 2015.

[4] W.E. Alnaser and N.W. Alnaser, "The status of renewable energy in the GCC countries," **Renewable and Sustainable Energy Reviews**, vol. 15, pp. 3074-3098, 2011.

[5] B. R. Hughes, J. K. Calautit and S. A. Ghani, "The Development of Commercial Wind Towers for Natural Ventilation: a review," **Applied Energy**, vol. 92, pp. 606-627, 2011.

[6] D. O'Connor, J. K. Calautit and B. R. Hughes, "A Study of Passive Ventilation Integrated with Heat Recovery," **Energy and Buildings**, vol. 82, pp. 799-811, 2014.

[7] J. K. Calautit, B. R. Hughes, and S. A. Ghani, "A Numerical Investigation into the Feasibility of Integrating Green Building Technologies into Row Houses in the Middle East," **Architectural Science Review**, vol. 56, pp. 279-296, 2013.

[8] S. Attia and A. De Herde, "Designing the Malqaf for summer cooling in low-rise housing, an experimental study," **Conference on Passive and Low Energy Architecture**, Quebec City, Canada, pp. 22-24, 2009. 1989

[9] J. K. Calautit, B. R. Hughes and S. A. Ghani, "Numerical investigation of the integration of heat transfer devices into wind towers," **Chemical Engineering Transactions**, vol. 34, pp. 43-48, 2013.

[10] J. K. Calautit, H. N. Chaudhry, B. R. Hughes and S. A. Ghani, "Comparison between evaporative cooling and heat pipe assisted thermal loop for a commercial wind tower in hot and dry climatic conditions," **Applied Energy**, vol. 101, pp. 740-755, 2013.

[11] J. K. Calautit, B. R. Hughes , H. N. Chaudhry, and S. A. Ghani, "CFD analysis of a heat transfer device integrated wind tower system for hot and dry climate," **Applied Energy**, vol. 112, pp. 576-591, 2013.

[12] A.A. Badran, "Performance of cool towers under various climates in Jordan," **Energy and Buildings**, vol. 35, pp. 1031-1035, 2003.

[13] M. Bahadori, M. Mazidi and A. R, Dehghani, "Experimental investigation of new designs of wind towers," **Renewable Energy**, vol. 33, pp. 2273–2281, 2008.

[14] M.A. Yaghoubi, A. Sabzevari, A.A. Golneshan, ""Wind Towers - Measurement and Performance," **Solar Energy**, vol. 47, pp. 97-106, 1991.

[15] Y. Bouchahm, F. Bourbia and A. Belhamri, "Performance analysis and improvement of the use of wind tower in hot dry climate," **Renewable Energy**, vol. 36, pp. 898-906, 2011.

[16] H. Saffari and S. Hosseinnia, "Two-phase Euler-Lagrange CFD simulation of evaporative cooling in a Wind Tower," **Energy and Buildings**, vol. 41, pp. 991–1000, 2009.

[17] L. Shao and S.B. Riffat, "Flow loss caused by heat pipes in natural ventilation stacks," **Applied Thermal Engineering**, vol. 17, pp. 393-399, 1997.

[18] V. Kalantar, "Numerical simulation of cooling performance of wind tower (Baud-Geer) in hot and arid region," **Renewable Energy**, vol. 34, pp. 246–254, 2009.

[19] T Chung, Computational fluid dynamics, Cambridge University Press, vol. 1, pp. 15-21,

[20] J. K. Calautit and B. R. Hughes, "Measurement and prediction of the indoor airflow in a room ventilated with a commercial wind tower," **Energy and Buildings**, vol. 84, pp. 367-377, 2014.

[21] ANSYS® Academic Research. ANSYS FLUENT User's Guide Release 14.0. Pennsylvania: ANSYS, Inc; 2014
[22] B. R. Hughes, H. N. Chaudhry and J. K. Calautit,"Passive energy recovery from natural ventilation air streams," **Applied Energy**, vol. 113, pp.127-140, 2014.
[23] J. K. Calautit and B. R. Hughes, "Wind tunnel and CFD study of the natural ventilation performance of a commercial multi-directional wind tower," **Building and Environment**, vol. 80, pp. 71-83, 2014.
[24] J. K. Calautit, D. O'Connor and B. R. Hughes, "Determining the optimum spacing and arrangement for commercial wind towers for ventilation performance," **Building and Environment**, vol. 82, pp. 274-287, 2014.
[25] H. N. Chaudhry, J. K. Calautit and B. R. Hughes, "Computational analysis of a wind tower assisted passive cooling technology for the built environment," Journal of Building Engineering, vol. 1, pp. 63-71, 2015
[26] J. K. Calautit, H. N. Chaudhry, B. R. Hughes and L. F. Sim, ""A validated design methodology for a closed-loop subsonic wind tunnel," **Journal of Wind Engineering and Industrial Aerodynamics,** vol. 125, pp. 180-194, 2014.
[27] J. Cermak and N. Isyumov, Wind tunnel studies of buildings and structure, ASCE Publications, 1999.
[28] Windfinder. Wind & weather statistics Ras Al-Khaimah Airport, UAE, available in: http://www.windfinder.com/windstatistics/ras_al-khaimah_airport
[29] Z. Zhang, W. Zhang, Z. Zhai and Q. Chen, "Evaluation of Various Turbulence Models in Predicting Airflow and Turbulence in Enclosed Environments by CFD: Part 2—Comparison with Experimental Data from Literature," **HVAC and R Research**, vol.13, pp. 871-886, 2007
[30] Building Regulations 2000: Approved Document F1A: Means of Ventilation, NBS: London, 2010.
[31] J. K. Calautit, D. O'Connor and B. R. Hughes, "A natural ventilation wind tower with heat pipe heat recovery for cold climates," **Renewable Energy**, 2015, http://dx.doi.org/10.1016/j.renene.2015.08.026.
[32] Building Bulletin, Building Bulletin 98: Briefing Framework for Secondary School Projects, 2004.

Nomenclature

u	velocity magnitude (m/s)
X, Y, Z	Cartesian co-ordinates (m)
Re	Reynolds number
ρ	air density (kg/m^3)
μ	kinematic viscosity (m^2/s)
Q	volume flow rate (m^3/s)
g	gravitational acceleration (m/s^2)
A	cross-sectional area (m^2)
ΔP	total pressure loss (Pa)
P	pressure (Pa)
P_o	total pressure (Pa)
P_s	static pressure (Pa)
L	length (m)
W	width (m)
H	height (m)
t	time (sec)

Figure 1 Different forms of traditional wind catcher architecture [5].

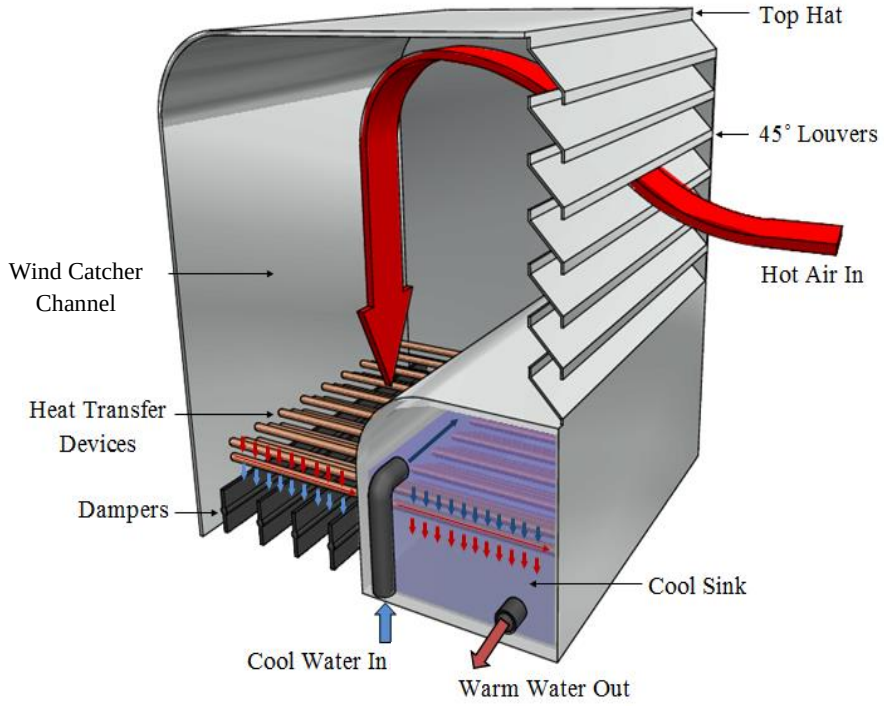

Figure 2 Cooling wind catcher with heat pipes.

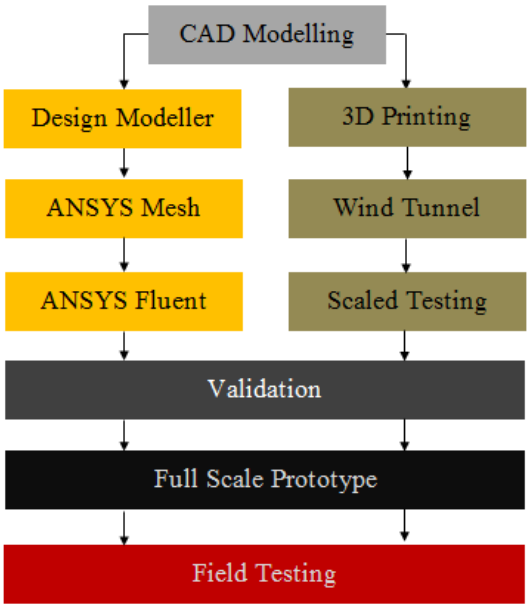

Figure 3 Research methodology flow chart.

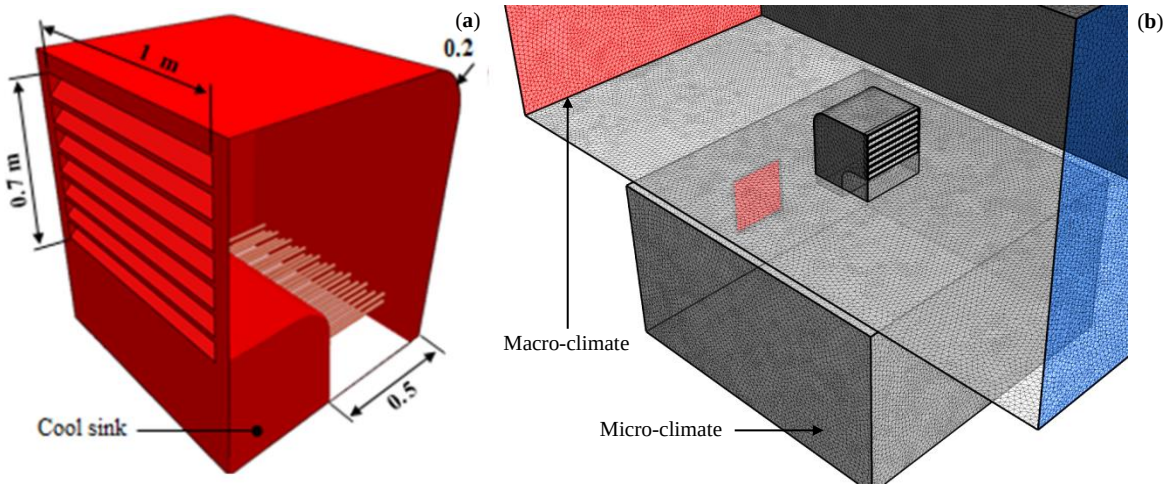

Figure 4 (a) CAD model of the wind catcher with cylindrical heat pipes (b) Computational mesh of the wind catcher and test room model.

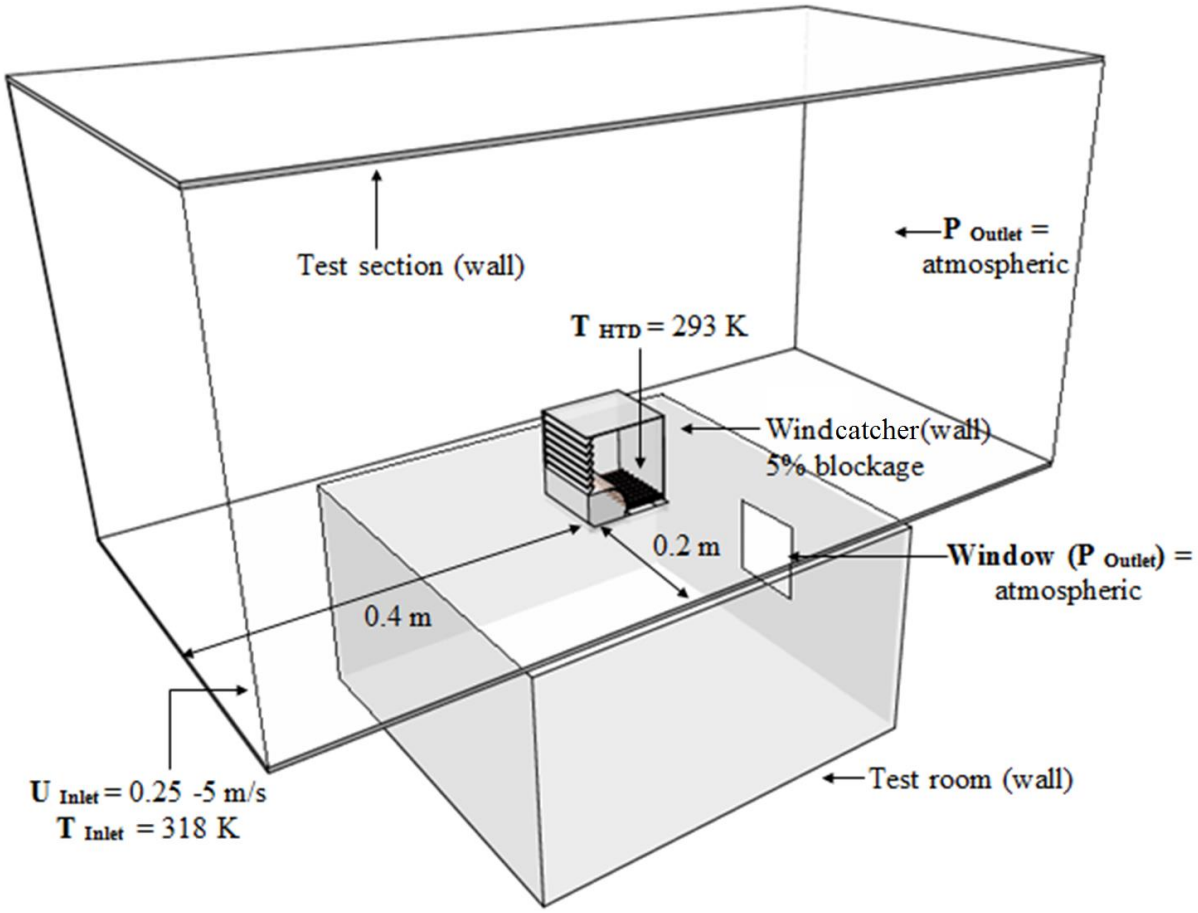

Figure 5 Computational domain showing the set boundary conditions.

Figure 6 Wind tunnel test setup.

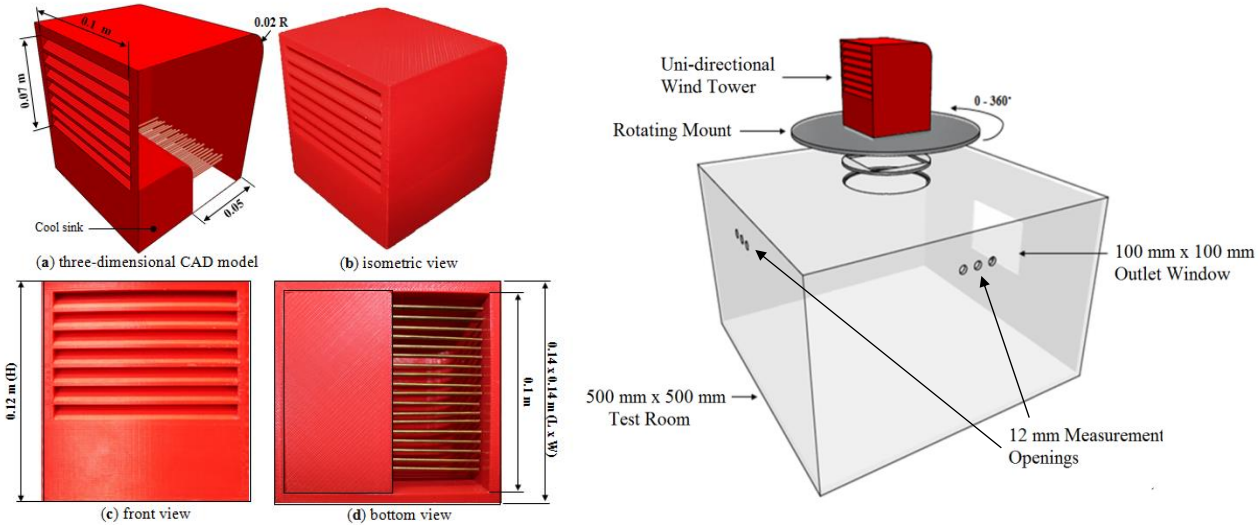

Figure 7 (a) Schematic diagram of the wind catcher with cylindrical heat pipes (b) test room.

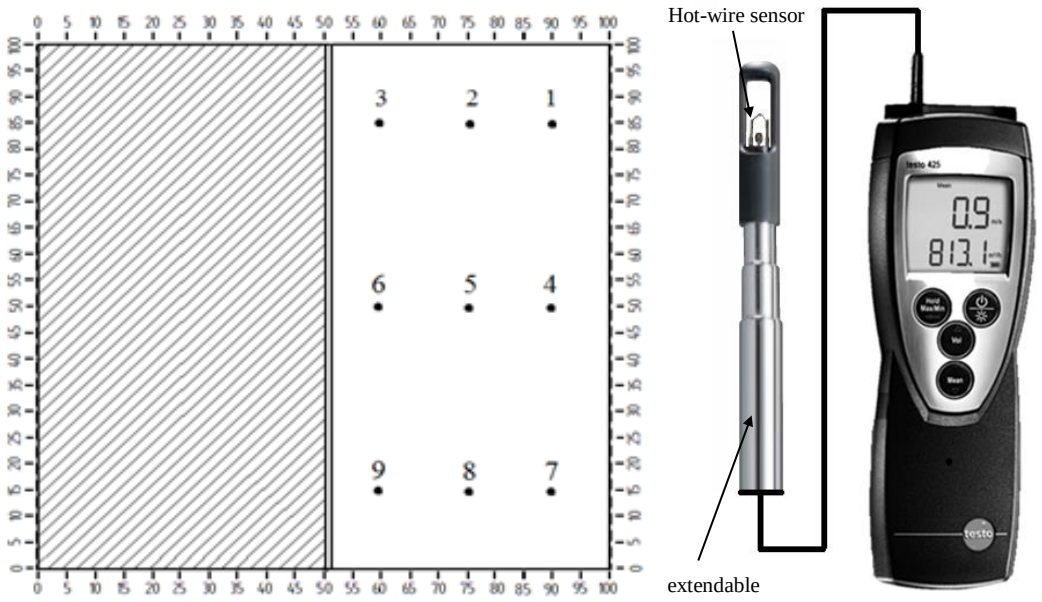

Figure 8 (a) Location of measurement points below the wind catcher channel (b) hot-wire anemometer.

Figure 9 Field test site in Ras Al Khaimah, UAE.

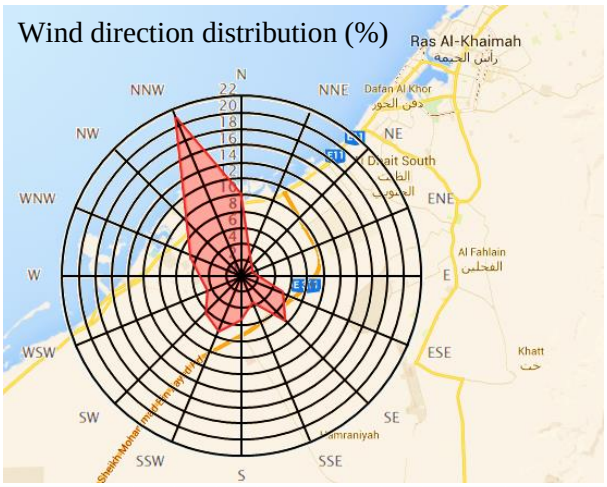

Month of year	Jan	Feb	Mar	Apr	May	Jun	Jul	Aug	Sep	Oct	Nov	Dec	Year
	01	02	03	04	05	06	07	08	09	10	11	12	1-12
Dominant Wind dir.													
Average Wind speed (m/s)	4	4	4	4	5	4	4	5	4	4	4	4	4
Average air temp. (°C)	20	21	25	32	36	37	39	38	36	32	27	23	30

Figure 10 Weather data of Ras Al Khaimah, UAE [28].

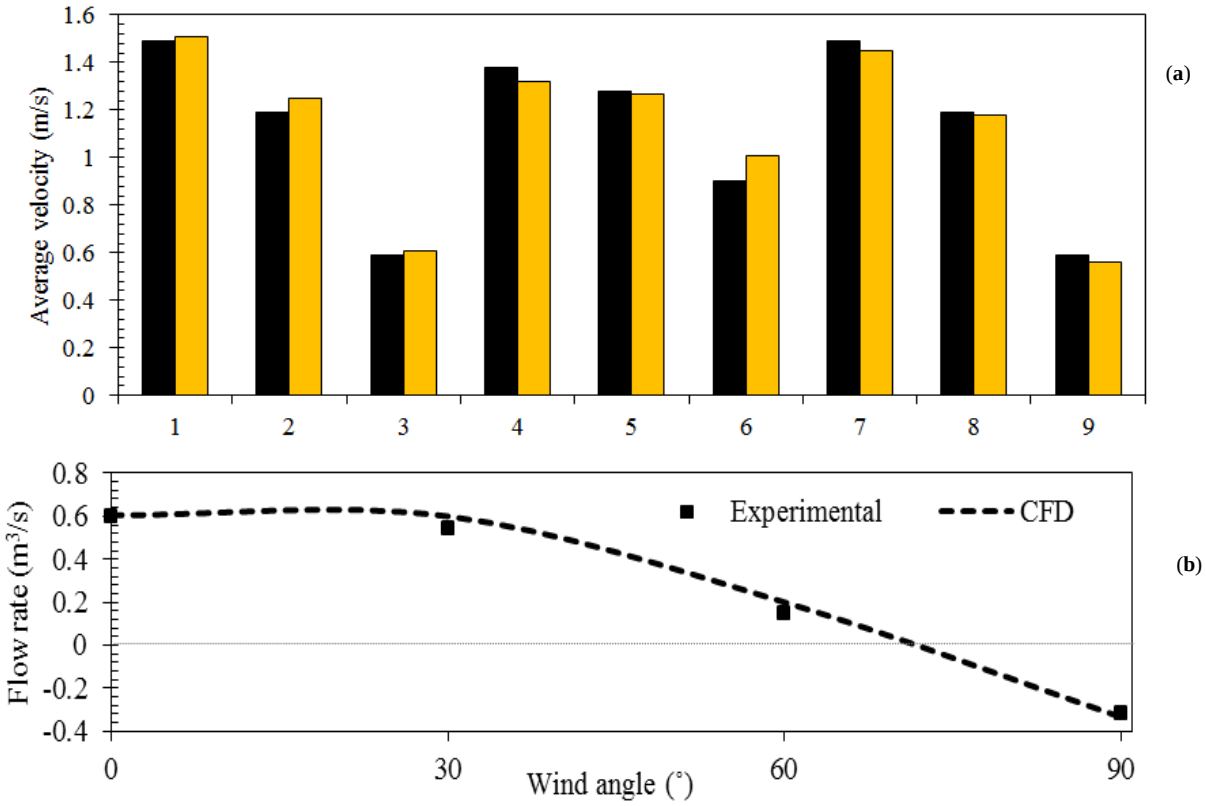

Figure 11 (a) Comparison between CFD and experimental results of the (a) velocity in the supply channel (b) effect of variation of wind direction on the supply flow rate.

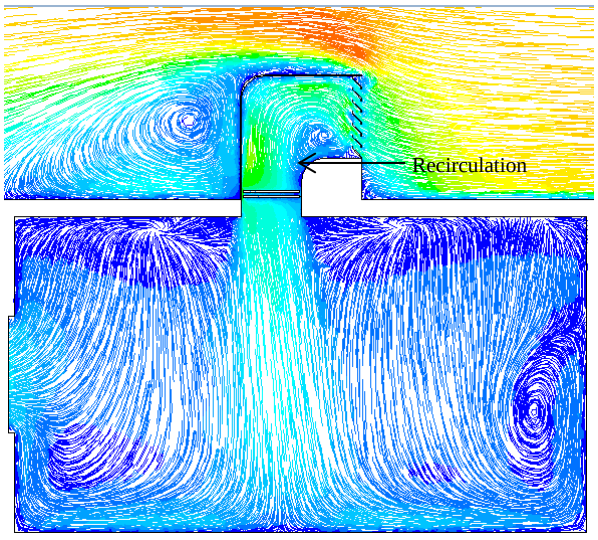

Figure 12 CFD streamlines showing indoor

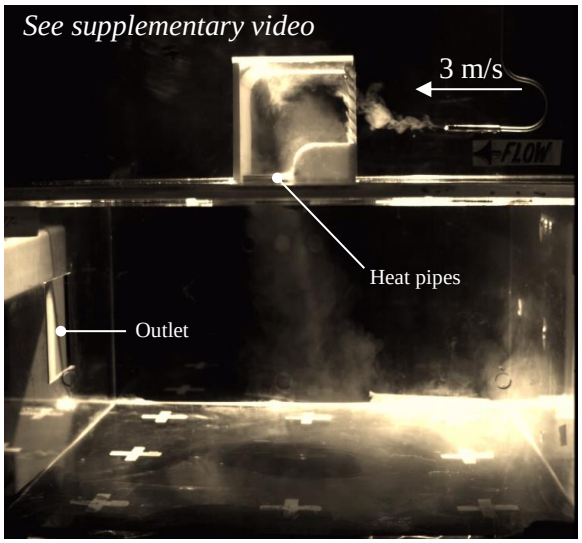

Video 1 Experimental flow visualisation

airflow distribution inside the test room with the wind catcher.

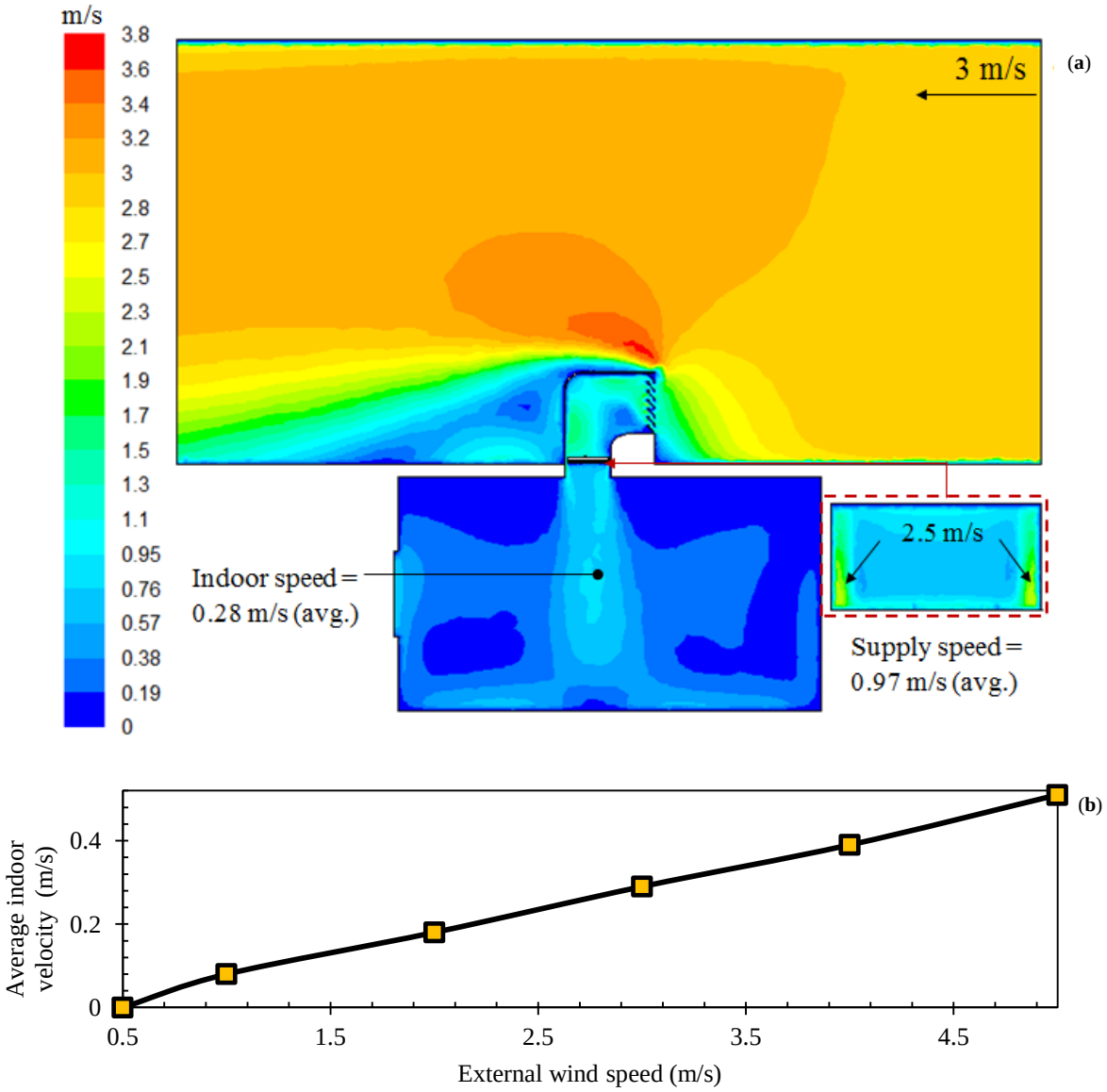

Figure 13 (a) Contours of airflow velocity in vertical cross-sectional plane (b) effect of increasing wind speed on internal airflow distribution.

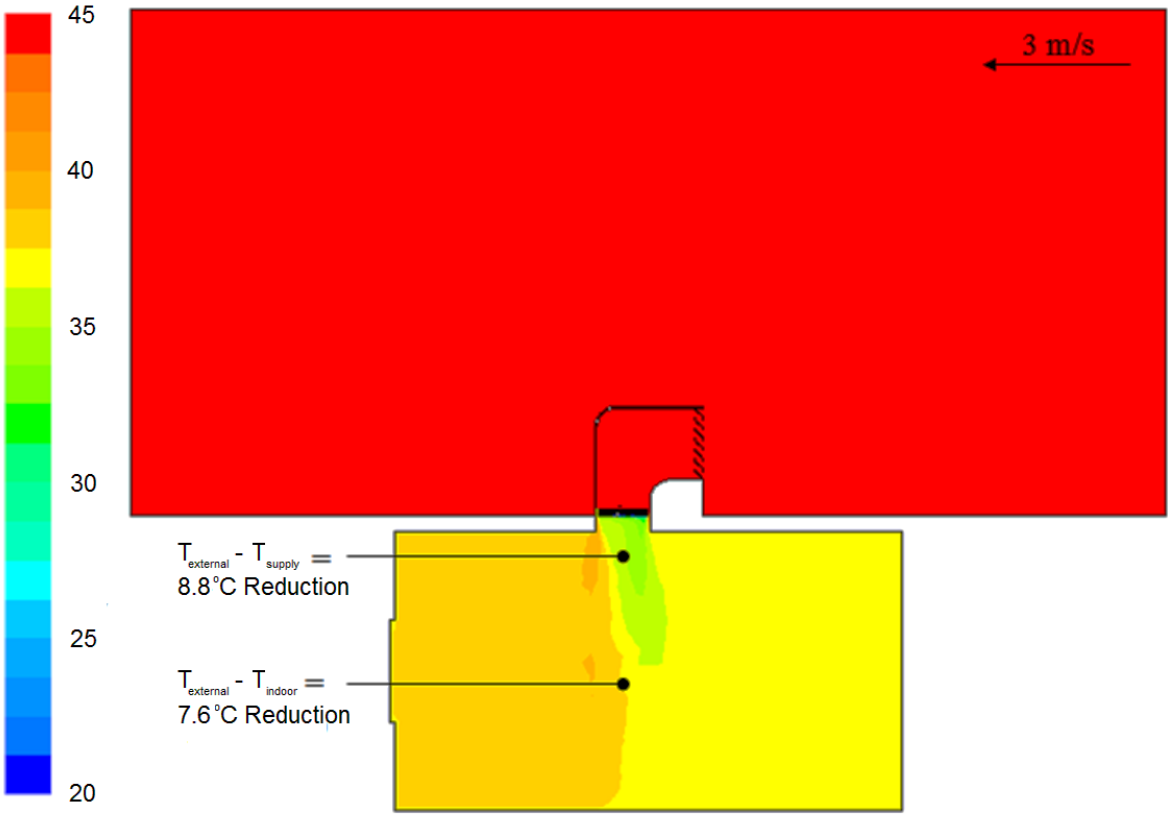

Figure 14 Contours of airflow temperature in vertical cross-sectional plane.

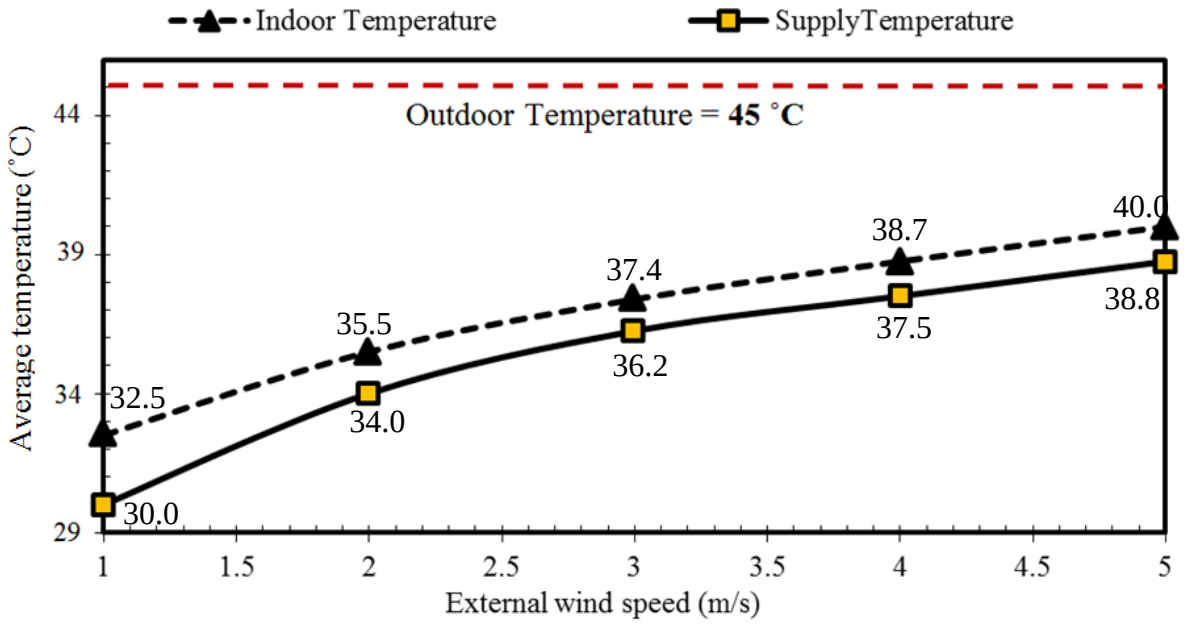

Figure 15 Effect of increasing wind speed on internal and supply air temperature.

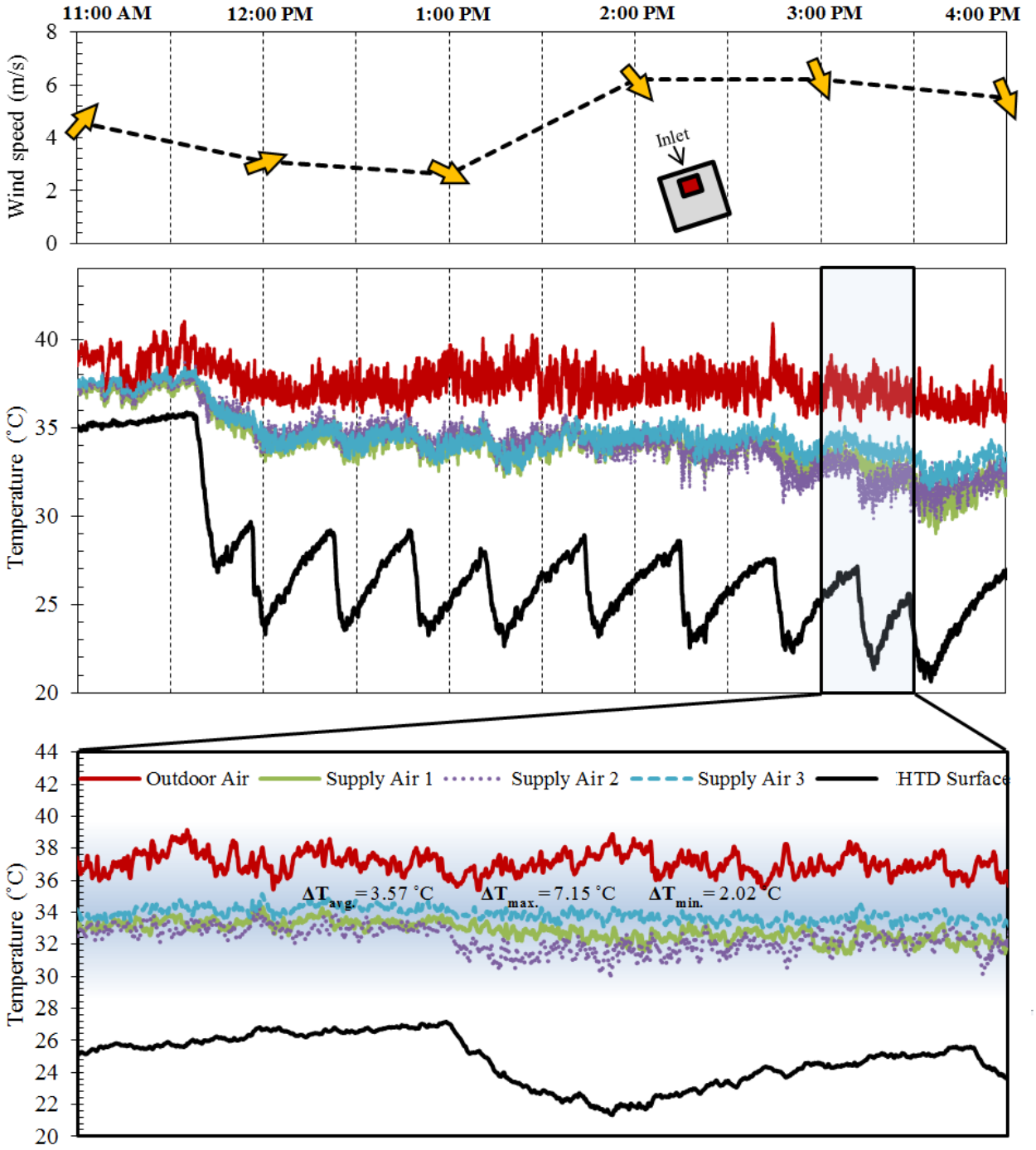

Figure 16 September 17, 2014 testing: (a) Wind speed and direction (b) Heat pipe surface, outdoor air and supply air temperature (c) temperature results from 3:00 PM to 3:30 PM.

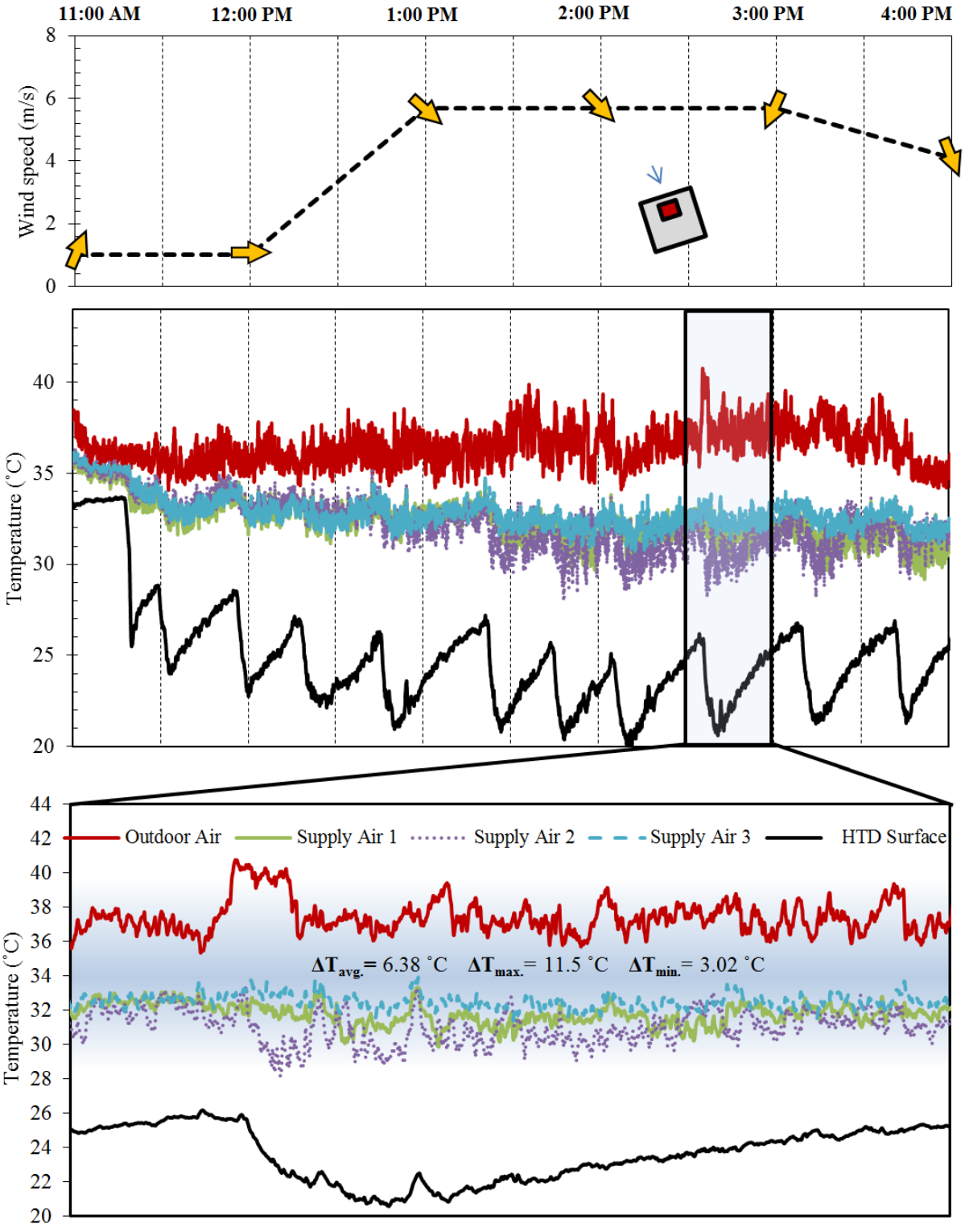

Figure 17 September 18, 2014 testing: (a) Wind speed and direction (b) Heat pipe surface, outdoor air and supply air temperature (c) temperature results from 2:30 PM to 3:00 PM.

Table 1 Calculated ventilation rates for various external wind speeds.

Wind speed [m/s]	Supply rate L/s	L/s/occupant	L/s/m^2
0.50	65.00	**4.33**	2.60
1.00	145.00	**9.67**	5.80
2.00	325.00	21.67	13.00
3.00	485.00	32.33	19.40
4.00	695.00	46.33	27.80
5.00	840.00	56.00	33.60